2018 European Control Conference (ECC)
June 12-15, 2018. Limassol, Cyprus

A Control Strategy for Variable-Speed Variable-Pitch Wind Turbines within the regions of partial- and full-load operation without wind speed feedback

L. Cavanini[2], M.L. Corradini[1], G. Ippoliti[2], G. Orlando[2]

Abstract— **In this paper, the control of a variable-speed variable-pitch wind turbine in the whole wind speed range is addressed, without any feedback measurement of wind speed. An aerodynamic torque observer is adopted to ensure the tracking of the Maximum Delivered Power in the partial-load region, while a novel wind speed observer is proposed for power regulation in the full-load region, along with a novel sliding surface ensuring finite-time set-point stabilization of the speed tracking error. Transitions between regions can be seen as changes in the reference to be tracked by the generator electrical torque and by the blades pitch angle. The proposed control solution has been validated on the National Renewable Energy Laboratory (NREL)** $5-MW$ **three-blade wind turbine model.**

I. Introduction

Wind Turbines (WT) are one of the fastest growing power generation solutions due to abundance of wind energy, little negative impact on environment and advancement of supporting technologies. To meet the growing demand, wind turbines are being scaled up both in size and power rating and have to operate in time-varying wind speed, where operation and control change significantly along the wind speed range [1]. The extraction of wind power by a Wind Energy Conversion System (WECS) can be divided in different operating regions associated with wind speed, maximum allowable rotor speed and rated power [2], [3]. In practice, variable-rotor-speed/variable-blade-pitch wind turbines have three main regions of operation with respect to wind speed [3]–[6]. A stopped turbine or a turbine that is just starting up is considered to be operating in region 1. Region 2 (partial-load region) is an operational mode with the objective of maximizing wind energy capture. In region 3 (full-load region), which encompasses high wind speeds, the control has to regulate the turbine at rated power limiting the captured wind power so that safe electrical and mechanical loads are not exceeded.

The control approach used by the wind industry to design of wind turbine control strategies for the entire operation envelope is based on two different controllers that can be designed to achieve the control goals under partial- and full-load operation, the optimization of their transition being an open problem [7]. In order to design controllers for wind turbines that covers the entire operating regions, generator torque control is usually used in region 2, while control of blade pitch is typically used to limit power and speed for turbines operating in region 3. Generator torque, and blade pitch strategies can all be used to shed excess power and limit the energy capture in region 3 but it is common to use only generator torque in region 2, keeping the blade pitch constant at an optimal value for peak energy extraction [8], [9].

The most basic approach uses a look-up-table in low wind speeds to achieve maximum energy capture, and a PI controller or a gain scheduling-based PI controller in high wind speeds to regulate the rotational speed [8], [10]. However, advanced control techniques have being exploited to design high performance wind turbine controllers, and a comprehensive overview of variable speed wind energy conversion systems is reported in [1]. For instance, nonlinear, optimal, fuzzy logic, neural network-based, adaptive, and sliding mode control strategies have been recently reported in the literature [11]–[16]. Most of the proposals are confined to either partial- [14], [15], [17] or full-load [18]–[20] operation, while only a few cover a wide operating range [11], [12], [16], [21]–[23]. Among the most advanced wind turbine control techniques for whole wind speed range, the linear parameter varying (LPV) gain scheduling approach is receiving great attention [7], [24].

The availability of reliable wind speed measurements, or its estimates, is a key factor for improving closed-loop control performances [19]. In region 3, the closed loop response could be potentially improved in terms of pitch sensitivity due to its dependence on wind speed. Indeed, wind speed is both the input for the system and the parameterizing variable for the dynamics that determine the operating point of the WECS [25] in the design procedure of a model-based wind turbine controller. To compensate for variations in parameters or dynamic behavior, adaptive or gain-scheduled controllers have been used, in which the control gains are adapted/scheduled based on the measured or calculated varying parameters [26], [27], such as the generator velocity in region 2 and the pitch angle in region 3 [24]. Using the wind speed as scheduling parameter would have an advantage of keeping a single parameter for the whole operation region [28] but the measured wind speed

[1]M.L. Corradini is with Scuola di Scienze e Tecnologie, Università di Camerino, via Madonna delle Carceri, 62032 Camerino (MC), Italy letizia.corradini@unicam.it

[2]L. Cavanini, G. Ippoliti, G. Orlando are with the Dipartimento di Ingegneria dell'Informazione, Università Politecnica delle Marche, via Brecce Bianche, 60131 Ancona, Italy {l.cavanini, gianluca.ippoliti, giuseppe.orlando}@univpm.it

on the nacelle is unfortunately imprecise and not a good representative of the rotor effective wind speed [25]. To solve this problem, a number of algorithms present dedicated estimators of the wind speed affecting the entire rotor and a good comprehensive analysis of these techniques in given in [25]. Indeed, recent advances in light detection and ranging (LIDAR) systems have shown promise for providing real-time measurements of wind speed [29], opening a new area of research in feedforward wind turbine control [30], [31] and receding horizon control for load reduction [32]. It is worth recalling that, in general, sensors may be source of potentials faults, inaccuracies, poor performance, inefficient energy transfer.

In this paper, the regions of partial- and full-load operation have been considered under the assumption that no feedback information about wind speed is available. The proposed control scheme has a simple structure, and two controllers are used to manage the two operational modes and the natural transition between them. The objective of the control system is defined as that of maintaining the rotor speed and the pitch angle at suitable values depending on the region at which the turbine operates. For the rotor speed, the overall control problem can be seen as that of finding the reference electrical torques to be tracked. In this sense, transitions between regions can be simply seen as corresponding to changes in the electrical torque reference variable to be tracked. Analogously, for the pitch angle, transitions between regions corresponds to changes in the reference pitch angle to be tracked by means of the control variable applied to the pitch actuator. An aerodynamic torque observer is adopted in the proposed scheme to ensure the tracking of the Maximum Delivered Power in Region 2 [17], while a novel wind speed observer is proposed for power regulation in Region 3. For the same region 3, a novel sliding surface is proposed guaranteeing finite-time vanishing of the speed tracking error. The proposed strategy is verified by simulation using the standard NREL 5 MW wind turbine model.

The paper is organized as follows. The WECS dynamics are presented in Section 2, while in Section 3 the aero-dynamical torque observer is recalled and the control law ensuring the MDP tracking is presented. In Section 4, the fixed-time control law for full-load operation is given in the general case, along with details about the wind speed observer design. Results on numerical tests are reported in Section 5. The paper ends with comments about the proposed control policy.

II. WECS Dynamics

The system model here reported is inspired by the studies [24], [33] and references therein. As well known, wind energy is transformed first into mechanical energy through the WT blades and, ultimately, into electrical energy through the generator. The aerodynamic (mechanical) power that the wind turbine extracts from the wind is expressed by the following equation [24], [33]:

$$P_a = \frac{1}{2}\rho\pi r^2 C_p\left(\lambda,\beta\right)V(t)^3 \tag{1}$$

where ρ is the air density, r is the wind turbine rotor radius, V is the wind speed and the power coefficient $C_p\left(\lambda,\beta\right)$ represents the turbine efficiency to convert the kinetic energy of the wind into mechanical energy [24]. This coefficient is a function of both the blade pitch angle β and the tip speed ratio λ which is defined as [34] $\lambda = \frac{\omega}{V}r$, where ω is the WT angular shaft speed. The introduction of the expression of λ in Eq. (1) gives:

$$P_a = \frac{K_a r\omega C_p\left(\lambda,\beta\right)}{\lambda}V(t)^2 \tag{2}$$

with $K_a \stackrel{\text{def}}{=} \rho\frac{\pi}{2}r^2$. As a consequence, the torque that the wind turbine extracts from the wind is given by:

$$T_a(t) = \frac{K_a r C_p\left(\lambda,\beta\right)}{\lambda}V(t)^2. \tag{3}$$

The power coefficient $C_p\left(\lambda,\beta\right)$ is a nonlinear function [35], [36], and depends on blade aerodynamic design and WT operating conditions. In [33], the following equation is proposed to approximate the power coefficient for operation in region 2 ($\beta = 0\ deg$):

$$C_p\left(\lambda\right) = c_1\left(\frac{c_2}{\lambda_1} - c_4\right)e^{-\frac{c_5}{\lambda_1}} + c_6\lambda \tag{4}$$

$$\frac{1}{\lambda_1} = \left(\frac{1}{\lambda} - 0.035\right). \tag{5}$$

and $c_1 = 0.5176$, $c_2 = 116$, $c_4 = 5$, $c_5 = 21$, $c_6 = 0.0068$. In the same paper [33], the following equation is proposed to approximate the power coefficient in region 3:

$$C_p\left(\lambda,\beta\right) = c_1\left(k_1\gamma + k_2\beta + \bar{k}_3\right)\exp(k_4\gamma) \tag{6}$$

$$\gamma = \left(\frac{1}{\lambda + 0.08\beta} - \frac{0.035}{\beta^3 + 1}\right) \tag{7}$$

The following coefficient values have been considered for operation in region 3 [19]: $c_1 = 6.909$; $k_1 = 7.022$; $k_2 = -0.04176$; $\bar{k}_3 = -0.3863$; $k_4 = -14.52$. These coefficients have been obtained fitting the Eq. (6) to the C_p tables for the NREL $5-MW$ wind turbine generated using the NREL code WT_perf [19].

The mechanical equation governing the turbine can be simplified as follows [37]:

$$J\dot{\omega}(t) = -K\omega(t) + T_a(t) - N_g\tilde{T}_e(t) \tag{8}$$

where $\omega(t)$ is the rotor angular speed, K is the coefficients of viscous friction of the low-speed shaft, N_g is the gearbox ratio, $\tilde{T}_e(t)$ is the electrical torque of the generator. For convenience the following definition is introduced, to be used hereafter $T_e(t) \stackrel{\text{def}}{=} N_g\tilde{T}_e(t)$.

III. Region 2: variable speed and fixed pitch regime

In this section, a generator torque control with constant blade pitch to maximize energy capture of a variable-speed wind turbine operating in region 2 is considered [24]. This

control strategy is commonly used in commercial WTs operating under low and medium wind speeds, and the control objective is to achieve the maximum power coefficient C_{pmax} regardless of the wind speed. In particular, considering the definition of the tip speed ratio λ, at any wind speed within the operating range, there is a unique wind-turbine shaft rotational speed to achieve the maximum power coefficient C_{pmax}. From Eq. (3), when C_p is controlled at the maximum value, the maximum mechanical power is extracted from the wind energy. In other words, the generated power must follow the Maximum Delivered Power (MDP) characteristic for different wind speeds.

In region 2, the considered WT operates with a constant pitch angle $\beta = 0\ deg$ and the maximum power coefficient $C_{pmax} = 0.48$ is achieved for a tip speed ratio value $\lambda_{opt} = 7.5$. Thus, the optimal WT angular shaft speed is given by:

$$\omega_{ro} = \frac{\lambda_{opt} V}{r}. \tag{9}$$

Conventional techniques of turbine torque control scheme use wind speed measurements to determine the rotor reference torque [38], but this technique has some significant drawbacks [24] [2]. A modified version of the torque control scheme is here used, consisting in tracking the C_{pmax} locus in the low and medium wind speed region [24], [39] where the turbine has to operate at the peak of its C_p curve. It is worth noting that, in the standard version of the control scheme, the measured turbine speed ω_r is used to determine the optimum aerodynamic torque, deduced from Eq. (3) in MDP mode:

$$T_{opt} = \frac{1}{2}\frac{\rho \pi r^5 C_{p\max}}{\lambda_{opt}^3}\omega_r^2 = k_o \omega_r^2 \tag{10}$$

This T_{opt} is imposed as the reference torque T_e^* [4], [40] under the unrealistic assumption that the dynamical behavior of the WECS is neglectable. On the contrary, in the used sensorless control strategy [17], the tracking of the optimum aerodynamic torque is achieved without wind measurements and without the discussed oversimplifications.

A. The Aerodynamic Torque Observer

As already discussed in [17], a robust observer of the aerodynamic torque can be designed, able to ensure that the maximum efficiency is achieved (i.e. that $T_a = T_{opt}$ (10)), in the presence of bounded uncertainties affecting the coefficients of the mechanical model of the WECS, largely inaccurate, and without a direct measurement of wind speed. In other words, this subsystem provides as output the value of T_e, such that the peak of the C_p curve is tracked. Define the variables

$$\eta(t) = \int_0^t T_a(\tau)d\tau; \quad \bar{\eta}_{opt}(t) = \int_0^t \bar{k}_o \omega_r(t)^2(\tau)d\tau$$
$$\eta_{opt}(t) = \int_0^t k_o(\tau)\omega_r(t)^2(\tau)d\tau = \int_0^t T_{opt}(\tau)d\tau;$$

and consider the following observer:

$$\dot{\hat{\eta}}(t) = K\omega_r(t) + T_e(t) \tag{11}$$

where $\hat{\eta}(t)$ is the estimate of the variable $\eta(t)$. The following result can be proved:

Theorem 1: [17] The observer (11) is able to guarantee the robust vanishing of the error variables $\eta(t) - \eta_{opt}(t)$ and $\eta(t) - \hat{\eta}(t)$ for a suitable choice of the variable $T_e(t)$.

IV. Region 3: variable rotor speed and variable blade pitch WT regime

A. Characterization of the optimal rotor speed ω_r^* and the optimal blade pitch angle β^*

In the high wind speed region, the optimal rotor speed is the rated constant speed ω^* ensuring the achievement of the rated electrical power by the generator, depending on the size of the turbine and on the generator. The control problem becomes simply a set point stabilization problem. With reference to this region, it has been proved in [19] that the following expression for the reference pitch angle $\beta^*(V)$ provides a good estimate of the optimal value minimizing the squared error between the actual and the rated aerodynamical power:

$$\beta^*(V) = a_\beta V + b_\beta \stackrel{\text{def}}{=} 1.2998V - 8.2824\ [deg] \tag{12}$$

$\beta^*(V)$ depending only on the wind speed V expressed in $[m/s]$. When in the medium wind speed region, the optimal pitch angle is zero. Finally it should be recalled that, according to [41], the blade pitch actuator can be modeled as a first order lag:

$$\dot{\beta}(t) = -\frac{1}{\tau}\beta(t) + u(t) \tag{13}$$

where $u(t)$ is the control input, i.e. the torque supplied by the blade pitch actuator.

B. A wind speed observer

To avoid the need of accurate wind speed measurements required for the tracking of the reference pitch angle $\beta^*(V)$, a wind speed observer will be now proposed. The idea is that of designing a wind speed observer $\hat{V}(t)$ such that the aerodynamic power P_a is as close al possible to the rated one $\bar{P}_a$ when the rated speed ω_r^* is tracked, i.e. such that the following Lyapunov function

$$W = \left|\bar{P}_a - K_a C_p \hat{V}^3\right| \tag{14}$$

is considered in region 3, with $K_a = \frac{\pi}{2}\rho R^2$. Deriving (14), one gets that the condition $\dot{W} < 0$ is ensured by the following expression

$$\dot{\hat{V}} = \gamma\left(\frac{\partial C_p}{\partial \hat{V}}\hat{V} + 3C_p\right) sign(\bar{P}_a - K_a C_p \hat{V}^3); \quad \gamma > 0. \tag{15}$$

In order to find a suitable expression of C_p, the expression of the power coefficient for $\omega(t) = \omega_r^*$ has been interpolated with the following best-fit polynomial of degree 3 with respect to β (in degrees) and 1 with respect to V, obtaining

$$C_p = \gamma_0 + \gamma_{10}V + \gamma_{01}\beta + \gamma_{11}V\beta + \gamma_{02}\beta^2 + \gamma_{03}\beta^3 \tag{16}$$

with $\gamma_0 = 0.7058$, $\gamma_{10} = -0.0306$, $\gamma_{01} = -0.0542$, $\gamma_{11} = 0.0020$, $\gamma_{02} = 0.0037$, $\gamma_{03} = -1.16\ 10^{-4}$ in the case of the considered reference $5MW$ NREL [8] wind turbine ($\omega_r^* = 1.2m/s$).

C. A sliding surface ensuring finite time stabilization

Finite-time setpoint stabilization of the speed tracking error $\omega(t) - \omega_r^*$ for the plant (8) will be here addressed, with the extra requirement that the settling time is upper bounded by an a-priori value not dependent of the initial condition $\mathbf{x}(0)$. A novel terminal sliding surface will be designed with respect to the standard form of the terminal sliding surface, traditionally chosen as [42]:

$$s(t) = x_2(t) + \alpha x_1(t)^{m/n} + \beta x_1(t)^{p/q} \tag{17}$$

with proper constraints on the positive integers m, n, p, q.

The plant (8) can be rewritten as the following continuous-time, time invariant, uncertain second order plant described by:

$$\dot{\theta}(t) = \dot{x}_1(t) = x_2(t) = \omega(t) \tag{18}$$

$$\dot{\omega}(t) = \dot{x}_2(t) = f(\mathbf{x}) + v(t) + d(\mathbf{x}) \tag{19}$$

where: $\mathbf{x}(t) = [x_1(t)\ x_2(t)]^T = [\theta\ \omega]^T \in \mathbb{R}^2$ is the state vector (assumed available for measurement), $v(t) \in \mathbb{R}$ is the control input, $f(\mathbf{x}) : \mathbb{R}^2 \to \mathbb{R}$ is a sufficiently smooth vector fields satisfying $f(0) = 0$ over the domain of interest, and the uncertain term $d(\mathbf{x})$ summarizes eventual matched parameter variations and/or external disturbances affecting the system.

Assumption 1: The uncertain term $d(\mathbf{x})$ is bounded by a known function $\rho(\mathbf{x})$:

$$|d(\mathbf{x})| \leq \rho(\mathbf{x}) \tag{20}$$

Consider the following sliding variable

$$s(\mathbf{x}) = x_2(t) + 2\beta_1 \sqrt{|\arctan(x_1(t))|}(1 + x_1^2(t))\sigma(x_1(t)) \tag{21}$$

with $\sigma(x_1(t)) = sign(x_1(t))$, having redefined the sign function as follows:

$$sign(z) = \begin{cases} -1 & if\ z < 0 \\ 1 & if\ z \geq 0 \end{cases}$$

The following Theorem immediately follows:

Theorem 2: With reference to the 2-dimensional uncertain system (8) satisfying Assumption 1, the achievement of a sliding motion on the surface $s(\mathbf{x}) = 0$ guarantees the robust finite-time stabilization of the plant. Once the sliding surface is reached, the states reach the origin within a fixed time:

$$T_2 \leq \frac{1}{\beta_1}\sqrt{\frac{\pi}{2}} \tag{22}$$

Proof Once a sliding motion is established on the surface $s(\mathbf{x}) = 0$, the dynamics of the variable $x_1(t)$ are given by:

$$\dot{x}_1(t) = -2\beta_1 \sqrt{|\arctan(x_1(t))|}(1 + x_1^2(t))\sigma(x_1(t)) \tag{23}$$

Consider the case $x_1(t) \geq 0 \Leftrightarrow \arctan(x_1(t)) \geq 0$. It holds

$$x_1(t)\dot{x}_1(t) = -2\beta_1 \sqrt{\arctan(x_1(t))}(1 + x_1^2(t)) < 0 \tag{24}$$

and the solution of (24) satifies

$$\sqrt{\arctan(x_1(t))} - \sqrt{\arctan(x_1(0))} = -\beta_1 t \tag{25}$$

this proving that the settling time is given by

$$T_2(x_1(t)) = \frac{1}{\beta_1}\sqrt{\arctan(x_1(0))} \leq \frac{1}{\beta_1}\sqrt{\frac{\pi}{2}} \tag{26}$$

Analogous considerations can be derived in the case $x_1(t) < 0$, and the statement follows. ◇

D. A unified Lyapunov function

In order to pursue the control objectives previously described for operation in region 3, the error system is first defined with $e_\beta(t) = \beta(t) - \beta(t)^*$, $e_2(t) = \omega(t) - \omega_r^*$ and correspondingly $e_1(t) = \theta(t) - \theta(t)^* = \int_0^t \omega_r^* d\tau$. The following sliding surface is introduced

$$s(\mathbf{x}) = e_2(t) + 2\beta_1 \sqrt{|\arctan(e_1(t))|}(1 + e_1^2(t))\sigma(e_1) \tag{27}$$

and the following overall Lyapunov function is considered:

$$W_1 = W + \frac{1}{2}s(\mathbf{x})^2 + \frac{1}{2}|\beta - \beta^*(\hat{V})| \tag{28}$$

Considering each term, and imposing $\dot{W}_1 < 0$, one can easily see that the control input needed for the establishment of a sliding motion on $s(\mathbf{x}) = 0$ has the form

$$T_e(t) = \left[K\omega(t) + \beta_1 \frac{h''(e1)}{h'(e_1)^2} e_2(t) \quad -\frac{K_a V_M^3}{\omega(t)} sign(s(\mathbf{x})) \right] \tag{29}$$

where $V_M = \max(V)$ is the maximum allowed wind speed, along with

$$u(t) = \frac{1}{\tau}\beta(t) - \rho_2 a_\beta |\dot{\hat{V}}(t)| sign\left[\beta(t) - \beta^*(\hat{V})\right]; \tag{30}$$

where $\rho_2 > 1$,

$$h(x_1) = \sqrt{|\arctan(e_1)|} \tag{31}$$

and

$$h'(z) \stackrel{\text{def}}{=} \frac{\partial h(z)}{\partial z} \quad h''(z) \stackrel{\text{def}}{=} \frac{\partial h'(z)}{\partial z}. \tag{32}$$

V. Simulation tests

The proposed controller has been tested by intensive simulations. The main parameters of the considered WECS have been derived from [8] for the NREL 5 MW wind turbine. Validation tests have been performed using the FAST wind data shown in Fig. 3(a) [43], with turbulence 10% and mean value $10\ m/s$. Initial conditions have been set as $\omega_r(0) = 8.5\ rpm$, $\beta(0) = 0\,\text{deg}$. According to [8], the transition between region 2 and 3 has been set to occur when the rotor speed exceeds the value $1.1875\ rad/s$, and saturation of the electrical torque has been assumed to occur at $4500\ KNm$. Some of the performed tests have been reported in the following pictures. In particular, Fig. 1(a) and 1(b) show the electrical power and the rotor angular speed, respectively. It can be noted that, as expected, the power is maintained close to the rated value $\bar{P}_a = 5.29661MW$ in Region 3.

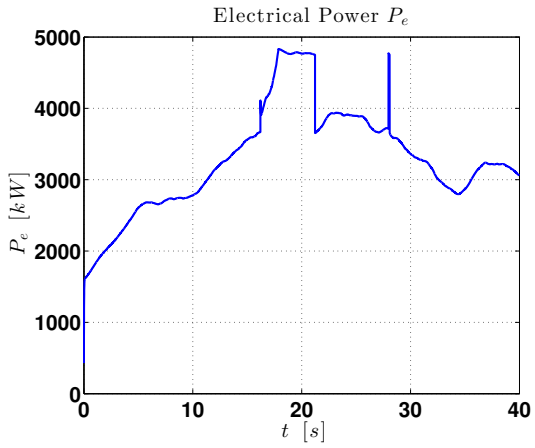

(a)

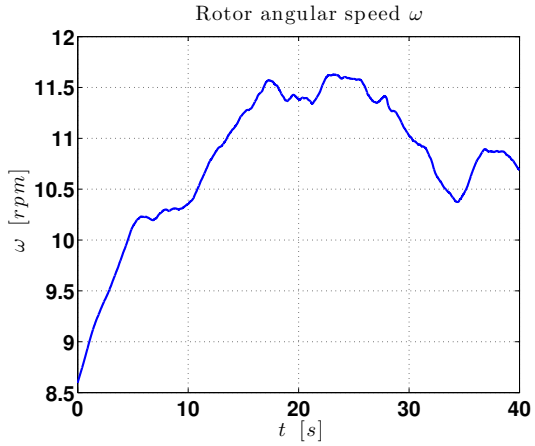

(b)

Fig. 1. (a) Electrical Power; (b) Rotor angular speed.

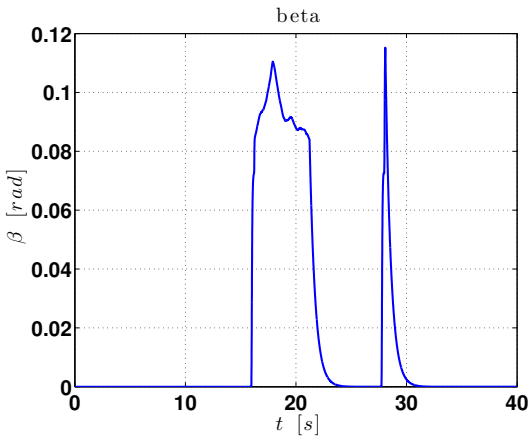

(a)

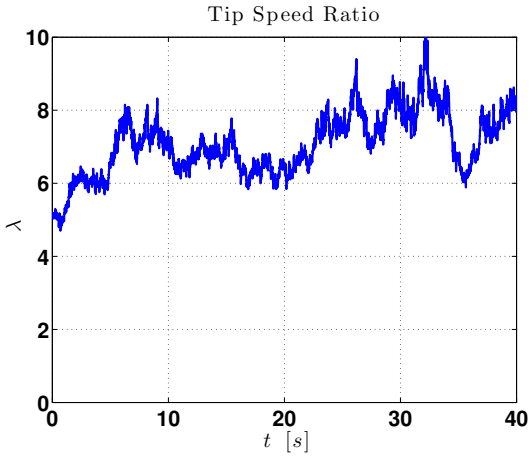

(b)

Fig. 2. (a) Blade pitch angular position; (b) Tip Speed Ratio.

Fig.2(a) shows the blade pitch angular position. The performance achieved in terms of efficiency of transferred energy is testified by results reported in Fig.2(b), showing that the tip speed ratio is close to its optimal value in region 2, and is far from its optimal value when the transition to high wind speeds occurs. The behavior of the wind speed observer is reported in Fig. 3(a), along with the actual wind speed sequence used for the simulation.

VI. Conclusions

This paper addresses the control of wind turbines within the complete wind speed velocity range, and presents a control strategy enriching the wind industry widely accepted two-step design with advanced control techniques.In particular, a robust observer of the aerodynamic torque is employed to track the MDP in region 2 without a direct measurement of the wind speed. In region 3, the tracking of the reference blade pitch angle is based on a wind speed observer and control algorithm ensuring the finite-time vanishing of the rotor speed error. A unified Lyapunov function has been design to pursue these control objectives in region 3. A simulation study based on the NREL 5-MW wind turbine has been reported.

References

[1] J. G. Njiri and D. Soffker, "State-of-the-art in wind turbine control: Trends and challenges," *Renewable and Sustainable Energy Reviews*, vol. 60, pp. 377 – 393, 2016.

[2] B. Beltran, T. Ahmed-Ali, and M. Benbouzid, "High-order sliding-mode control of variable-speed wind turbines," *IEEE Trans. Ind. Electron.*, vol. 56, no. 9, pp. 3314 –3321, 2009.

[3] M. Liserre, R. Cardenas, M. Molinas, and J. Rodriguez, "Overview of Multi-MW wind turbines and wind parks," *IEEE Trans. on Industrial Electronics*, vol. 58, no. 4, pp. 1081–1095, April 2011.

[4] K. Johnson, L. Pao, M. Balas, and L. Fingersh, "Control of variable-speed wind turbines: standard and adaptive techniques for maximizing energy capture," *IEEE Contr. Sys. Mag.*, vol. 26, no. 3, pp. 70 – 81, 2006.

[5] M. Cirrincione, M. Pucci, and G. Vitale, "Neural MPPT of variable-pitch wind generators with induction machines in a wide wind speed range," *IEEE Trans. on Industry Applications*, vol. 49, no. 2, pp. 942–953, March 2013.

[6] T. Senjyu, R. Sakamoto, N. Urasaki, T. Funabashi, H. Fujita, and H. Sekine, "Output power leveling of wind turbine generator for all operating regions by pitch angle control," *IEEE Trans. on Energy Conversion*, vol. 21, no. 2, pp. 467–475, June 2006.

[7] F. A. Inthamoussou, F. D. Bianchi, H. D. Battista, and R. J. Mantz, "LPV wind turbine control with anti-windup features covering the complete wind speed range," *IEEE Trans. on Energy Conversion*, vol. 29, no. 1, pp. 259–266, March 2014.

[8] J. Jonkman, S. Butterfield, W. Musial, and G. Scott, "Definition of a 5-MW Reference Wind Turbine for Offshore System Development,"

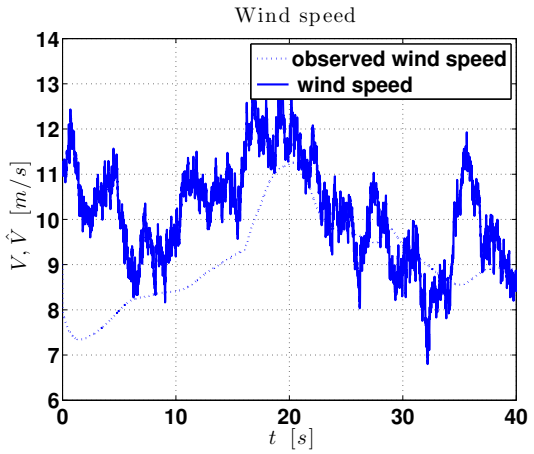

(a)

Fig. 3. (a) Wind Inflow (green line) along with the output of the wind speed observer (15) (dotted line);

NREL, Colorado, Tech. Rep. NREL/TP-500-38060, February 2009. [Online]. Available: http://www.nrel.gov/docs/fy09osti/38060.pdf

[9] L. Y. Pao and K. Johnson, "Control of wind turbines," *IEEE Control Systems*, vol. 31, no. 2, pp. 44–62, April 2011.

[10] E. A. Bossanyi, "Wind turbine control for load reduction," *Wind Energy*, vol. 6, no. 3, pp. 229–244, 2003.

[11] R. Sakamoto, T. Senjyu, N. Urasaki, T. Funabashi, H. Fujita, and H. Sekine, "Output power leveling of wind turbine generators using pitch angle control for all operating regions in wind farm," *Proc. 13th Int. Conf. on Intelligent Systems Application to Power Systems*, 2005.

[12] H. Geng and G. Yang, "Output power control for variable-speed variable-pitch wind generation systems," *IEEE Trans. on Energy Conversion*, vol. 25, no. 2, pp. 494–503, June 2010.

[13] R. Vepa, "Nonlinear, optimal control of a wind turbine generator," *IEEE Trans. on Energy Conversion*, vol. 26, no. 2, pp. 468–478, June 2011.

[14] W. Meng, Q. Yang, Y. Ying, Y. Sun, Z. Yang, and Y. Sun, "Adaptive power capture control of variable-speed wind energy conversion systems with guaranteed transient and steady-state performance," *IEEE Trans. on Energy Conversion*, vol. 28, no. 3, pp. 716–725, Sept 2013.

[15] C. Evangelista, F. Valenciaga, and P. Puleston, "Active and reactive power control for wind turbine based on a mimo 2-sliding mode algorithm with variable gains," *IEEE Trans. on Energy Conversion*, vol. 28, no. 3, pp. 682–689, Sept 2013.

[16] H. Jafarnejadsani, J. Pieper, and J. Ehlers, "Adaptive control of a variable-speed variable-pitch wind turbine using radial-basis function neural network," *IEEE Trans. on Control Systems Technology*, vol. 21, no. 6, pp. 2264–2272, Nov 2013.

[17] M. Corradini, G. Ippoliti, and G. Orlando, "Robust control of variable-speed wind turbines based on an aerodynamic torque observer," *IEEE Trans. Contr. Syst. Technol.*, vol. 21, no. 4, pp. 1199–1206, 2013.

[18] A. Uehara, A. Pratap, T. Goya, T. Senjyu, A. Yona, N. Urasaki, and T. Funabashi, "A coordinated control method to smooth wind power fluctuations of a pmsg-based wecs," *IEEE Trans. on Energy Conversion*, vol. 26, no. 2, pp. 550–558, June 2011.

[19] M. Corradini, G. Ippoliti, and G. Orlando, "Observer-based blade-pitch controller of wind turbines in high wind speeds," *Control Engineering Practice*, vol. 58, no. 1, pp. 186–192, 2017.

[20] F. Bianchi, R. Mantz, and C. Christiansen, "Power regulation in pitch-controlled variable-speed WECS above rated wind speed," *Renewable Energy*, vol. 29, no. 11, pp. 1911 – 1922, 2004.

[21] G. Semrau, S. Rimkus, and T. Das, "Nonlinear systems analysis and control of variable speed wind turbines for multiregime operation," *ASME. J. Dyn. Sys., Meas., Control.*, vol. 137, no. 4, pp. 041 007–041 007–10, April 2015.

[22] R. Saravanakumar and D. Jena, "Validation of an integral sliding mode control for optimal control of a three blade variable speed variable pitch wind turbine," *International Journal of Electrical Power & Energy Systems*, vol. 69, pp. 421 – 429, 2015.

[23] J. Chen, J. Chen, and C. Gong, "New overall power control strategy for variable-speed fixed-pitch wind turbines within the whole wind velocity range," *IEEE Trans. on Industrial Electronics*, vol. 60, no. 7, pp. 2652–2660, July 2013.

[24] F. D. Bianchi, H. N. D. Battista, and R. J. Mantz, *Wind Turbine Control Systems: Principles, Modelling and Gain Scheduling Design*. Berlin: Springer-Verlag, 2007.

[25] M. Soltani, T. Knudsen, M. Svenstrup, R. Wisniewski, P. Brath, R. Ortega, and K. Johnson, "Estimation of rotor effective wind speed: A comparison," *IEEE Trans. on Control Systems Technology*, vol. 21, no. 4, pp. 1155–1167, July 2013.

[26] F. D. Bianchi, R. J. Mantz, and C. F. Christiansen, "Control of variable-speed wind turbines by LPV gain scheduling," *Wind Energy*, vol. 7, no. 1, pp. 1–8, 2004.

[27] D. J. Leith and W. E. Leithead, "Appropriate realization of gain-scheduled controllers with application to wind turbine regulation," *International Journal of Control*, vol. 65, no. 2, pp. 223–248, 1996.

[28] K. Ohtsubo and H. Kajiwara, "LPV technique for rotational speed control of wind turbines using measured wind speed," *Oceans '04. MTTS/IEEE Techno-Ocean '04*, vol. 4, pp. 1847–1853 Vol.4, Nov 2004.

[29] T. Mikkelsen, N. Angelou, K. Hansen, M. Sjöholm, M. Harris, C. Slinger, P. Hadley, R. Scullion, G. Ellis, and G. Vives, "A spinner-integrated wind lidar for enhanced wind turbine control," *Wind Energy*, vol. 16, no. 4, pp. 625–643, 2013.

[30] N. Wang, K. Johnson, and A. Wright, "FX-RLS-Based feedforward control for LIDAR-Enabled wind turbine load mitigation," *IEEE Trans. on Control Systems Technology*, vol. 20, no. 5, pp. 1212–1222, Sept 2012.

[31] ——, "Comparison of strategies for enhancing energy capture and reducing loads using LIDAR and feedforward control," *IEEE Trans. on Control Systems Technology*, vol. 21, no. 4, pp. 1129–1142, July 2013.

[32] M. Soltani, R. Wisniewski, P. Brath, and S. Boyd, "Load reduction of wind turbines using receding horizon control," *2011 IEEE Int. Conf. on Control Applications (CCA)*, pp. 852–857, Sept 2011.

[33] J. Zaragoza, J. Pou, A. Arias, C. Spiteri, E. Robles, and S. Ceballos, "Study and experimental verification of control tuning strategies in a variable speed wind energy conversion system," *Ren. Ener.*, vol. 36, no. 5, pp. 1421 – 1430, 2011.

[34] W. Qiao, L. Qu, and R. Harley, "Control of IPM synchronous generator for maximum wind power generation considering magnetic saturation," *IEEE Trans. Ind. Appl.*, vol. 45, no. 3, pp. 1095 –1105, 2009.

[35] A. Monroy and L. Alvarez-Icaza, "Real-time identification of wind turbine rotor power coefficient," *45th IEEE Conf. Dec. Contr.*, pp. 3690 –3695, 2006.

[36] H. Siegfried, *Grid integration of wind energy conversion systems*. John Wiley & Sons Ltd, 1998.

[37] J.M. Jonkman and M.L. Buhl , "FAST User's Guide," National Renewable Energy Laboratory, 1617 Cole Boulevard, Golden, Colorado, Tech. Rep. NREL/EL-500-38230, August 2005. [Online]. Available: http://wind.nrel.gov/public/bjonkman/TestPage/FAST.pdf

[38] R. Fernandez, R. Mantz, and P. Battaitotto, "Sliding mode control for efficiency optimization of wind electrical pumping systems," *Wind Ener.*, vol. 6, pp. 161–178, 2003.

[39] M. El-Mokadem, V. Courtecuisse, C. Saudemont, B. Robyns, and J. Deuse, "Experimental study of variable speed wind generator contribution to primary frequency control," *Ren. Ener.*, vol. 34, pp. 833 – 844, 2009.

[40] L. Pao and K. Johnson, "Control of wind turbines," *IEEE Contr. Sys. Mag.*, vol. 31, no. 2, pp. 44 –62, 2011.

[41] A. Stotsky, B. Egardt, and O. Carson, "Control of wind turbines: a tutorial on proactive perspectives," *Proc. 2013 Am. Control Conf.*, pp. 3429–3436, 2013.

[42] Z. Zuo, "Nonsingular fixed-time terminal sliding mode control of nonlinear systems," *IET Control Theory and applications*, vol. 9, pp. 545–552, 2014.

[43] NWTC, "NWTC Information Portal (FAST)," https://nwtc.nrel.gov/FAST, last modified 19-March-2015 ; Accessed 28-April-2016.